JLab PAC12 Proposal Cover Sheet

This document must be received by close of business on Thursday, June 26, 1997

Jefferson Lab
User Liaison Office, Mail Stop 12 B
12000 Jefferson Avenue
Newport News, VA 23606

(Choose one)

☒ New Proposal Title: Polarization Transfer in Kaon Electroproduction

☐ Update Experiment Number:

☐ Letter-of-Intent Title:

Contact Person

Name: O. Keith Baker
Institution: Hampton University and Jefferson Laboratory
Address: Department of Physics
Address: Hampton University
City, State, ZIP/Country: Hampton, VA 23668 USA
Phone: 757-727-5820 269-7343 Fax: 757-269-7363
E-Mail: baker@cebaf.gov

Experimental Hall: C Days Requested for Approval: 15

Jefferson Lab Use Only

Receipt Date: 6/26/97 97-007

By:

Polarization Transfer in Kaon Electroproduction: Collaboration

K. Assamagan, O.K. Baker (Spokesman)[!], T. Eden, P. Gueye, R. Madey, L. Tang[!], R. Williams
Hampton University, USA
[!]and, jointly, Thomas Jefferson National Accelerator Facility, USA

J. Dunne, R. Ent
Thomas Jefferson National Accelerator Facility, USA

C. Bennhold, K. Dhuga, T. Mart
George Washington University, USA

C.C. Chang
University of Maryland, USA

P. Markokwitz
Florida International University

J. Reinhold, B. Zeidman

Argonne National Laboratory, USA

S. Beedoe, S. Danagoulian, C. Jackson, S. Mtingwa, R. Sawafta
North Carolina A&T State University, USA

E. Cisbani, S. Frullani, F. Garibaldi, M. Iodice, G.M. Urcivoli
INFN, Rome

T. Saito
Tohoku University, Japan

TJNAF Proposal

Polarization Transfer in Kaon Electroproduction

Abstract

This proposal describes an experiment to study the mechanism of polarization transfer in kaon electroproduction. The physics goal is to extract information about the hyperon electromagnetic form factor at large momentum transfer. In the electromagnetic production of kaons from a proton, the associated Λ-hyperon will be identified by missing mass in the reaction, and the decay proton from the hyperon will be detected. Since the Λ-hyperon is self-analyzing, a determination of the proton momentum vector can be used to measure the hyperon spin polarization vector. Thus the experiment will serve to elucidate the process of polarization transfer from the polarized electron to the Λ-hyperon.

The polarization transfer response functions, $R_{TT'}$ and $R_{LT'}$ will be determined for squared momentum transfer, Q^2, from 0.4 to 2.1 $(GeV/c)^2$, with kaons (hyperons) detected along (opposite to) the momentum transfer direction (in the center of mass frame). In the laboratory frame, both kaon and hyperon momentum vectors lie parallel to the momentum transfer direction. The experiment will be carried out in Hall C using standard equipment; the HMS and SOS with the same detector packages as were used in the kaon electroproduction experiments which were completed in the fall of 1996, and the cryogenic (unpolarized) hydrogen target.

The response functions $R_{LT'}$ and $R_{TT'}$ exhibit sensitivity to the Λ-hyperon electromagnetic form factor at nonzero Q^2 ($Q^2 > 0$). Presently, this is the best way to measure hyperon form factors for large space-like momentum transfer. At the higher momentum transfers, the experimental data can shed light on the hyperon spin structure.

Overview

Strangeness electroproduction, that is, the electromagnetic production of hadronic systems with constituent strangeness, remains one of the forefront areas of research in nuclear and particle physics at intermediate energies. The CEBAF accelerator at TJNAF has proven to be a powerful tool for use in studying the electromagnetic production of hadronic systems containing a strange constituent quark. The electromagnetic probe only marginally disturbs the system being investigated, and is well understood [1-6]. Its use as a means to probe the internal structure of hadronic systems has been well documented. Among the most studied of these hadronic systems is the nucleon. The unique opportunities afforded by the use of polarized, high-current, high-duty-factor electron beams provides an even more powerful probe of the electromagnetic structure of hadronic systems; the study of the electromagnetic production and weak decay of the hyperon, specifically the Λ-hyperon, becomes feasible. This proposal describes an experiment to study the electroproduction of the Λ as a function of momentum transfer, angle, and energy, in order to extract insights into its production and weak decay dynamics.

The free Λ-hyperon has a lifetime, τ_Λ, of about 3×10^{-10} s; it exhibits two main decay modes, both mesonic:

$$\Lambda \rightarrow \mathrm{p} + \pi^- + 37.8 \text{ MeV } (0.642) \tag{O1}$$

$$\Lambda \rightarrow \mathrm{n} + \pi^\circ + 41.1 \text{ MeV } (0.358). \tag{O2}$$

Here the number in parenthesis shows the decay branching fraction. Consider the free decay of a Λ hyperon into a proton and pion. (Similar arguments apply to the decay into a neutron and neutral pion.) The proton and pion are emitted back-to-back in the Λ rest frame. Normally, it is not necessary to detect the pion in a Λ decay experiment in order to determine the decay mechanism because of these constraints (momentum conservation as well as the self-analyzing nature of the hyperon).

The current experiment aims to study the mechanism of polarization transfer in the reaction

$$\vec{e} + \mathrm{p} \rightarrow \mathrm{e}' + \mathrm{K}^+ + \vec{\Lambda}. \tag{O3}$$

A polarized electron beam and the existing cryogenic hydrogen target in Hall C are required. The experiment will use the HMS and SOS in Hall C to detect the scattered electron and the electroproduced kaon before it decays in flight, respectively. Additionally, the SOS will be used to detect the proton from the hyperon decay. The SOS used as a hyperon tagger, in general terms, will detect the protons resulting from the weak decays of the hyperons in

$$\vec{\Lambda} \rightarrow \mathrm{p} + \pi^-. \tag{O4}$$

The hyperon is self-analyzing; its polarization will be determined by measuring the angular distribution of the momenta of the protons (from the hyperon decays) with respect to the hyperons'. Both the kaon and the hyperon in this measurement will be detected along the virtual photon direction (in the laboratory frame). Thus the SOS will serve the dual

purpose of identifying the kaon electroproduction reaction as well as tagging the hyperon spin polarization vector. This is explained more carefully in the section on the experimental setup and procedure in this proposal.

The reaction to be studied, (O3), is kinematically complete in the Hall C setup. Once the momenta of the scattered electron and electroproduced kaon are measured, the hyperon momentum and energy are determined. Then, since the decay (O1) is well known, only the proton needs to be detected in the proposed measurement; the pion does not need to be detected. The hyperon momentum will be high enough so that the protons from the decay will lie in a rather tight cone centered on the hyperon momentum vector; the decay proton will be detected by the hyperon tagger (the SOS) for all hyperon spin directions (by a determination of the proton momentum). At the same time, the hyperon momentum will be low enough so that reasonable angular resolution can be achieved for proton detection in the reaction (O4). Time-of-flight measurement in the SOS will be used to identify the kaons and proton and to determine their momenta.

To lowest order in the fine structure constant $\alpha = e^2/4\pi \approx 1/137$, the electron interacts with the hadronic current through the exchange of a single virtual photon with well defined energy $\nu = \epsilon_i - \epsilon_f$ and momentum transfer $\vec{q} = -(\vec{k}_f - \vec{k}_i)$ Thus the kinematics of the electron scattering process is determined by three independent kinematical variables, usually chosen to be the invariant energy of the system, W, the scattering angle in the center of mass system θ, and the momentum transfer $Q^2 = -q^2$. The nucleon four-vectors are P=(E,$\vec{\mathrm{P}}$) for the initial and final states. It can be shown that the most general expression for a coincidence experiment considering an experiment with three types of polarization, target, beam, and recoil, is

$$\frac{\mathrm{d}\sigma}{\mathrm{d}\Omega_f \mathrm{d}\epsilon_f \mathrm{d}\Omega_K} = \Gamma \frac{\mathrm{d}\sigma_v}{\mathrm{d}\Omega_k} \tag{O5}$$

$$\frac{\mathrm{d}\sigma_v}{\mathrm{d}\Omega_k} = \frac{|k|}{k_\gamma^{cm}} P_\alpha P_\beta \{R_T^{\beta\alpha} + \epsilon_L R_L^{\beta\alpha} + [2\epsilon_L(1+\epsilon)]^{1/2}(R_{TL}^{\beta\alpha}\cos\phi_k + R_{TL}^{\beta\alpha}\sin\phi_k)$$

$$+\epsilon(R_{TT}^{\beta\alpha}\cos 2\phi_k + R_{TT}^{\beta\alpha}\sin 2\phi_k)$$

$$+h[2\epsilon_L(1-\epsilon)]^{1/2}(R_{TL'}^{\beta\alpha}\cos\phi_k + R_{TL'}^{\beta\alpha}\sin\phi_k) + h(1-\epsilon^2)^{1/2}R_{TT'}^{\beta\alpha}\} \tag{O6}$$

using the notation of reference [7] and Fig. (1). Here k denotes the electron momentum, P_α (P_β) is the magnitude of the target (recoil) polarization, the R's are the response functions with the superscripts α and β denoting the target and recoil polarization quantities, respectively, ϕ_k is the azimuthal angle between the electron scattering plane and the reaction plane, Γ is the virtual photon flux, and ϵ is the virtual photon polarization parameter. The response functions are bilinear combinations of the elementary amplitudes for kaon electroproduction. The expressions for these functions written in terms of the elementary amplitudes can be found in [2,7].

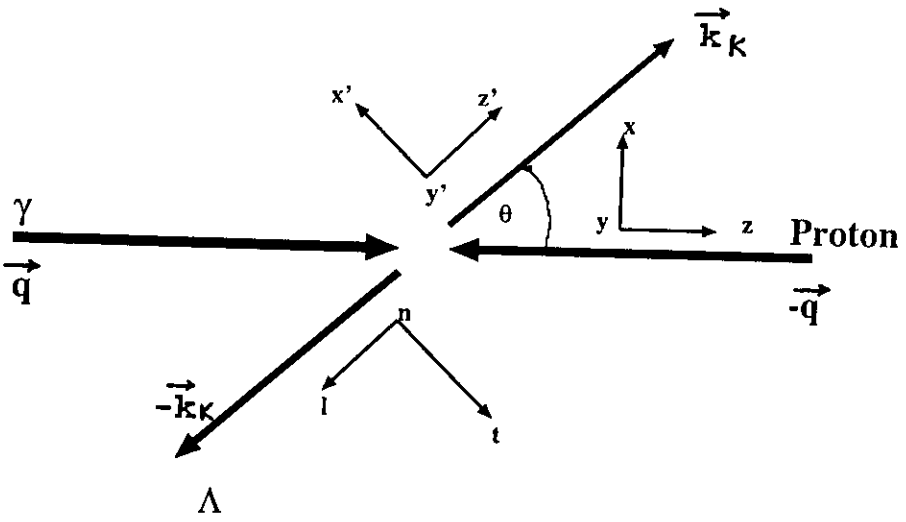

Figure (1). The kinematics of the polarization transfer reaction. Polarization gets transferred from the electron to the Λ hyperon with the emergent hyperon and kaon momenta lying along the momentum transfer direction.

In the specific case of polarized electron scattering (flipping the electron spin vector), no target polarization, and determination of the polarization of the decaying hyperon when the hyperon is detected along the q-vector, the equation reduces to

$$\frac{d\sigma_v^+}{d\Omega_k} - \frac{d\sigma_v^-}{d\Omega_k} = 2P_\beta \frac{|k|}{k_\gamma^{cm}}(1-\epsilon^2)^{1/2} R_{TT'}^{\beta 0}$$

$$= 2P_\beta \frac{|k|}{k_\gamma^{cm}}(1-\epsilon^2)^{1/2}({}^z R_{TT'}^{\beta 0} + {}^x R_{TT'}^{\beta 0}). \qquad (O7)$$

The $R_{TT'}$ response function will be measured at $Q^2 = 0.45$ to 2.06 $(GeV/c)^2$. The polarization transfer from a longitudinally polarized incident electron to a Λ hyperon which will then be longitudinally polarized in the same direction as the incident electron, will be determined in the experiment. In the kaon electroproduction reaction at these energies, the emergent Λ hyperon has a nonzero polarization (for $\theta_{k\gamma} \neq 0°$ or 180°). This induced polarization on the hyperon occurs for electroproduction with an unpolarized electron beam. The kinematics will be chosen such that the induced polarization will be zero for a

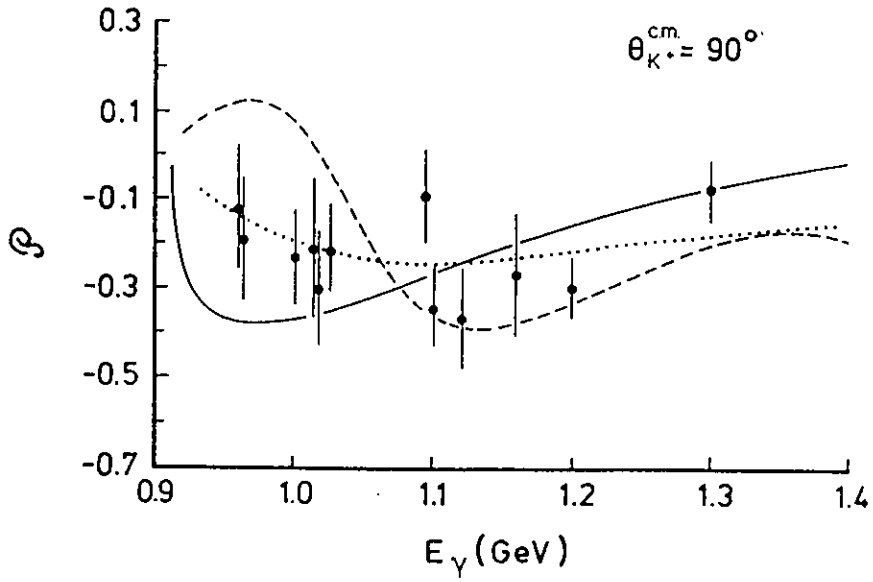

Figure (2). The <u>induced</u> polarization in the kaon electroproduction reaction (O3), from references [8-9]. The experiment described in this proposal will study polarization <u>transfer</u> as described in equation (O3) at smaller center of mass angles.

subset of the measurements (hyperon form factor determination), and nonzero in the subset of the data where desired (see Fig. (2)). The induced polarization vector lies in a plane which is orthogonal to the reaction plane (containing the hyperon momentum vector and the decay proton momentum vector). The polarization <u>transfer</u> vector lies in the reaction plane and will be orthogonal to the <u>induced</u> polarization vector. Both polarizations will be measured independently in the experiment. If there is a mechanism to produce interference between these two polarization mechanism, it can manifest itself by rotating either of these two polarization vectors from their orthogonal angle with respect to the other.

The CGLN formalism may be used to decompose the polarization response functions.

$$^{z}R^{\beta 0}_{TT'} = \mathrm{Re}\{-2F_1^*F_2 + \cos\theta(|F_1|^2 + |F_2|^2) - \sin^2\theta(F_1^*F_3 + F_2^*F_4)\} \qquad \text{(O8)}$$

$$^{x}R^{\beta 0}_{TT'} = \sin\theta\mathrm{Re}\{-|F_1|^2 + |F_2|^2 + F_2^*F_3 - F_1^*F_4 + \cos\theta(F_2^*F_4 - F_1^*F_3)\} \qquad \text{(O9)}$$

where θ is the angle between the virtual photon and kaon.

The unpolarized response functions due to transverse and longitudinal photons in the CGLN formalism are

$$R_T^{00} = \{|F_1|^2 + |F_2|^2 + \frac{\sin^2\theta}{2}(|F_3|^2 + |F_4|^2)$$

$$+\mathrm{Re}\{\sin^2\theta(F_2^*F_3 + F_1^*F_4 + \cos\theta F_3^*F_4) - 2\cos\theta F_1^*F_2\} \quad \text{(O10)}$$

and

$$R_L^{00} = \mathrm{Re}\{|F_5|^2 + |F_6|^2 + 2\cos\theta F_5^*F_6\} \quad \text{(O11)}$$

At $\theta_{K\gamma}$ equal to zero degrees, the expressions in (O8) and (O10) become, respectively,

$${}^zR_{TT'}^{\beta 0} = \mathrm{Re}\{-2F_1^*F_2 + (|F_1|^2 + |F_2|^2)\} \quad \text{(O12)}$$

and

$$R_T^{00} = |F_1|^2 + |F_2|^2 + \mathrm{Re}(-2F_1^*F_2) \quad \text{(O13)}$$

Combining the data from E93-018 where the longitudinal and transverse (unpolarized) response functions were measured and this proposed measurement of $R_{TT'}$ will give precise information on F_1 and F_2 separately. An example of how this will be achieved is as follows. Kaons will be detected in a narrow cone around $\theta_{K\gamma} = 0$ in the laboratory frame (corresponding to angles of up to 30° in the center of mass system). As the center of mass angle is increased from 0°, the difference between the response functions in equations (O8) and (O10) will be due almost entirely to the difference of $F_1^*F_2$ and $|F_1|^2 + |F_2|^2$. Therefore, this difference measured as a function of angle will allow extraction of these two amplitudes separately.

A similar analysis can be applied to gain information about the $R_{LT'}$ response function when appropriate binning of the data in ϕ_k along the virtual photon direction is performed offline. $R_{LT'}$ written in terms of the elementary amplitudes is

$${}^xR_{LT'}^{\beta 0} = \mathrm{Re}\{-F_2^*F_5 + F_1^*F_6 + \cos\theta(F_1^*F_5 - F_2^*F_6)\} \quad \text{(O14)}$$

$${}^zR_{LT'}^{\beta 0} = \sin\theta\mathrm{Re}\{F_1^*F_5 + F_2^*F_6\}. \quad \text{(O15)}$$

Along the momentum transfer direction,

$${}^xR_{LT'}^{\beta 0} = \mathrm{Re}\{-F_2^*F_5 + F_1^*F_6 + (F_1^*F_5 - F_2^*F_6)\} \quad \text{(O16)}$$

which when combined with the longitudinal response function measured in E93-018

$$R_L^{00} = \mathrm{Re}\{|F_5|^2 + |F_6|^2 + 2\cos\theta(F_5^*F_6)\} \quad \text{(O17)}$$

gives additional information for extracting the elementary CGLN amplitudes.

From these polarization transfer measurements, several physics issues can be studied in ways not feasible or even possible previously. Two examples are given in the following

section. The main physics motivation of the present experiment is the first measurement of the Λ-hyperon form factor at nonzero Q^2. This will be done by measuring the polarization transfer response functions given in equations (O8) and (O14) which are sensitive to this hyperon form factor.

Physics Motivation

Hyperon Internal Structure

There has been much recent interest in the study of the internal structure of baryons. Form factors are employed to describe the internal structure of hadronic systems [10-15]. Concurrently, nucleon form factors provide much needed, fundamental input for nucleon and nuclear structure models. The electric and magnetic form factors of neutrons and protons continue to be among the highest priority subjects in this field.

The marriage of these two subjects - strangeness electroproduction and nucleon form factors - results in a tantalizing new area for investigation, that of hyperon form factor measurements. The present proposal describes an experiment which is potentially sensitive to the electric and magnetic form factor of the Λ-hyperon at moderate momentum transfers. This information is fundamentally important in both nuclear and particle physics. The electroproduction of kaons with the associated production of hyperons (using polarization observables) is the most powerful means of extracting this information at large Q^2.

Presently, the only recoil polarization data in kaon electroproduction comes from the study of induced hyperon polarization [8-9,16] as shown in Fig. (2). (The kaon, being pseudoscalar, carries no spin polarization.) This experiment is the first proposed to study polarization transfer in the manner described in this proposal.

The earliest studies of the electromagnetic structure of the nucleons using moderate energy electromagnetic probes can be traced back to the work of Hofstadter and collaborators at Stanford [17]. It was shown that the electromagnetic probe interacts with the internal charge and current distribution of the nucleon - that is to say that the nucleons are not point objects, microscopically. The electromagnetic form factors are a measure of the deviation of these systems from pure point-like objects. The full momentum transfer dependence of these form factors cannot be calculated from first principles (quark and gluon degrees of freedom) over a large momentum transfer range. Experimental measurements combined with model calculations remain the only way to determine these quantities presently. Reasonable understanding of the internal structure of the baryons is necessary for progress in the field of intermediate energy nuclear and particle physics [18].

The most accurate experimental data that exists for nonzero momentum transfers is for the electric and magnetic form factors of the proton. Less precise data exists for the neutron. While these quantities have been measured reasonably well over a large momentum transfer region, there exists no data for the corresponding systems which contain a strange constituent quark, that is to say, hyperons.

The unique qualities of the CEBAF accelerator at TJNAF now make possible just such a measurement. This is a proposal to make a first measurement of the polarization transfer coefficient $R_{TT'}$ in kaon electroproduction. The polarization transfer from the electron to the hyperon in the reaction may be used to determine G_E^Λ and G_M^Λ, the Λ electric and magnetic form factors at nonzero momentum transfer.

The process to be studied is given by expression (O3) and (O4). The Feynman diagram of interest describing the process is shown in Fig. (3). The virtual photon from the electron scattering vertex couples directly to the Λ hyperon. Unfortunately, there are several other

processes which contribute to the experimental quantity measured, as shown in Figs. (4) and (5).

For most of the background processes which contribute, the polarization transfer mechanism provides a clean way for identification. These processes 'decay' into a kaon and hyperon. The maximum hyperon polarization in these processes combined is expected to be no more than 1/3 of the polarization transfer measured in the process of Fig. (3) [57]. The most insidious of the background processes is the coupling of the virtual photon to a Σ hyperon which then decays into Λ hyperon. The Σ hyperon is an isovector hadron as contrasted with the isoscalar Λ particle. Hence, one expects a different angular dependence for the process (see [19])

$$e + p \rightarrow e' + K^+ + \Lambda \qquad \text{(P1)}$$

compared to

$$e + p \rightarrow e' + K^+ + \Sigma. \qquad \text{(P2)}$$

Both Λ and Σ hyperons will be identified in the experiment. Then the ratio of the coupling to these two hyperons will be measured simultaneously. Experimental data confirms the theoretical prediction that the coupling the Σ-hyperon, $g_{KN\Sigma}$, is much weaker than the coupling to the Λ-hyperon, $g_{KN\Lambda}$, so the background process shown in Fig. (5) should not be difficult to handle.

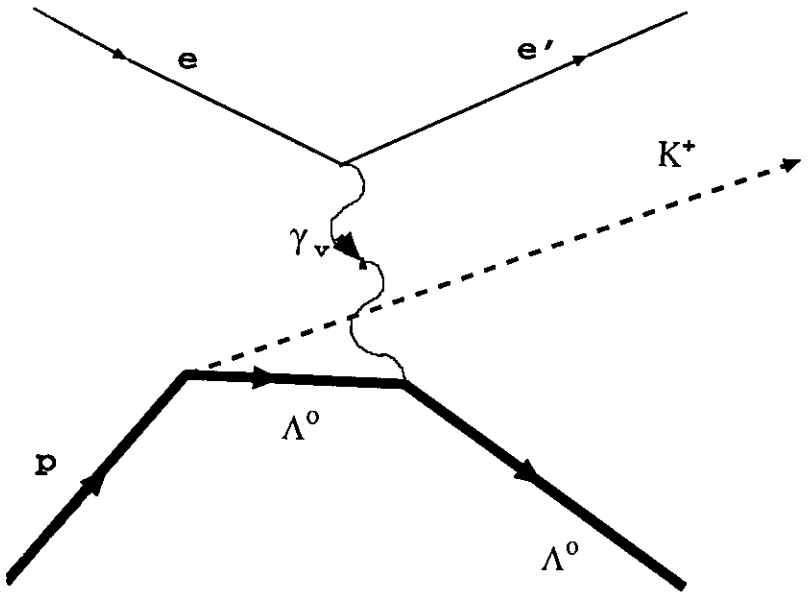

Figure (3). The Feynman diagram for the process of interest for the hyperon form factor. The virtual photon couples directly to the hyperon.

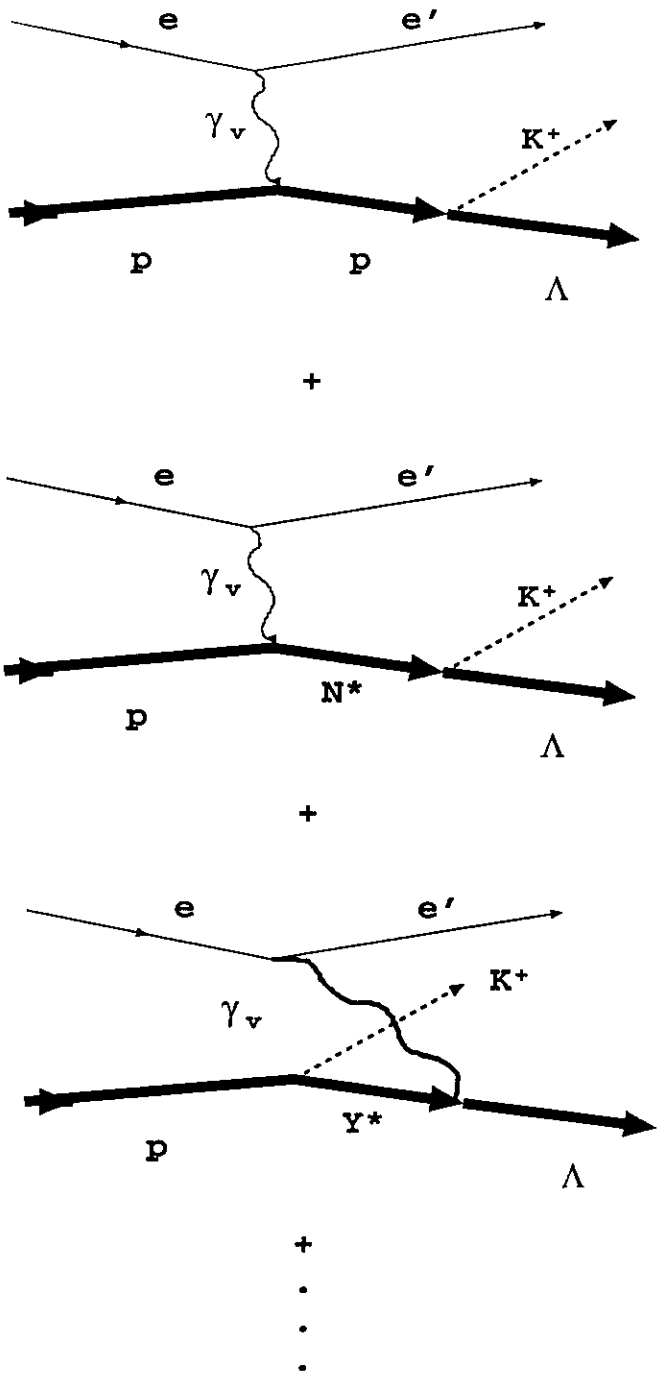

Figure (4). The Feynman diagrams for the background processes.

The Q^2 dependence of the polarization transfer response function $R_{TT'}^{z'0}$, is shown in Fig. (6). The curve is a calculation using the results of Williams for invariant energy (W) of 1.70 GeV, the same as will be used experimentally [20]. Also plotted on the curve is the expected precision of the measurement at the seven experimental points. It is reasonable

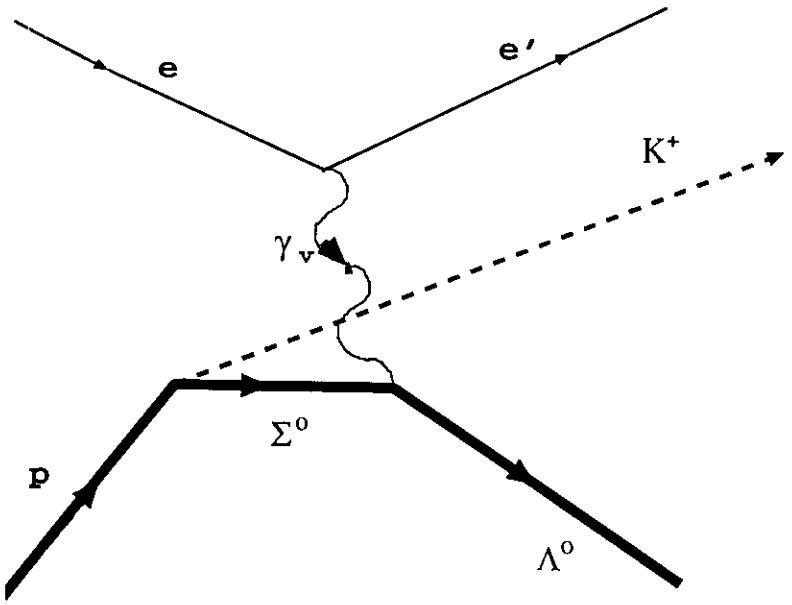

Figure (5).The most troublesome background process is when the virtual photon couples to the Σ hyperon which then converts to a Λ hyperon. The measurement of polarization transfer to the Λ will be used to separate these background processes whose coupling should be weak compared to the process shown in Fig. 3.

to expect a 5% precision as shown in the next section of this proposal. Fig. (7) shows the angular dependence of the response function for several different values of Q^2. In this experiment, only forward angle data ($\cos\theta_{cm} > 0.5$) will be gathered.

A calculation of the sensitivity of $R_{LT'}$ to the hyperon form factor versus squared momentum transfer is shown in Fig. (8) [58]. The sensitivity of $R_{TT'}$ to kaon, proton and hyperon form factor versus angle is given in Fig. (9). The calculation in Fig. (8) indicates that it is advantageous to make measurements at lower Q^2 values. The behavior competes against the expected Q^2 dependence of the hyperon form factors which are zero at $Q^2 = 0$ and with a small momentum transfer dependence.

The calculation shown in Fig. (9) illustrates the rate of change of $R_{TT'}$ with respect to the Λ, p, and K form factors versus the kaon center of mass production angle. The forward direction is where one can hope to select Λ and p form factors of comparable magnitude. It is worth noting that exactly at $\theta = 0°$ and $\theta = 180°$ the sensitivity to the kaon form factor is zero since the pseudoscalar kaon can carry no spin information in those cases. The calculation includes only Born diagrams with s and u channel resonances and excludes, for example, K* exchange in the t-channel process. This is justified on the basis of duality arguments [20].

Additionally, it has been shown that the electroproduction of fast hyperons along the

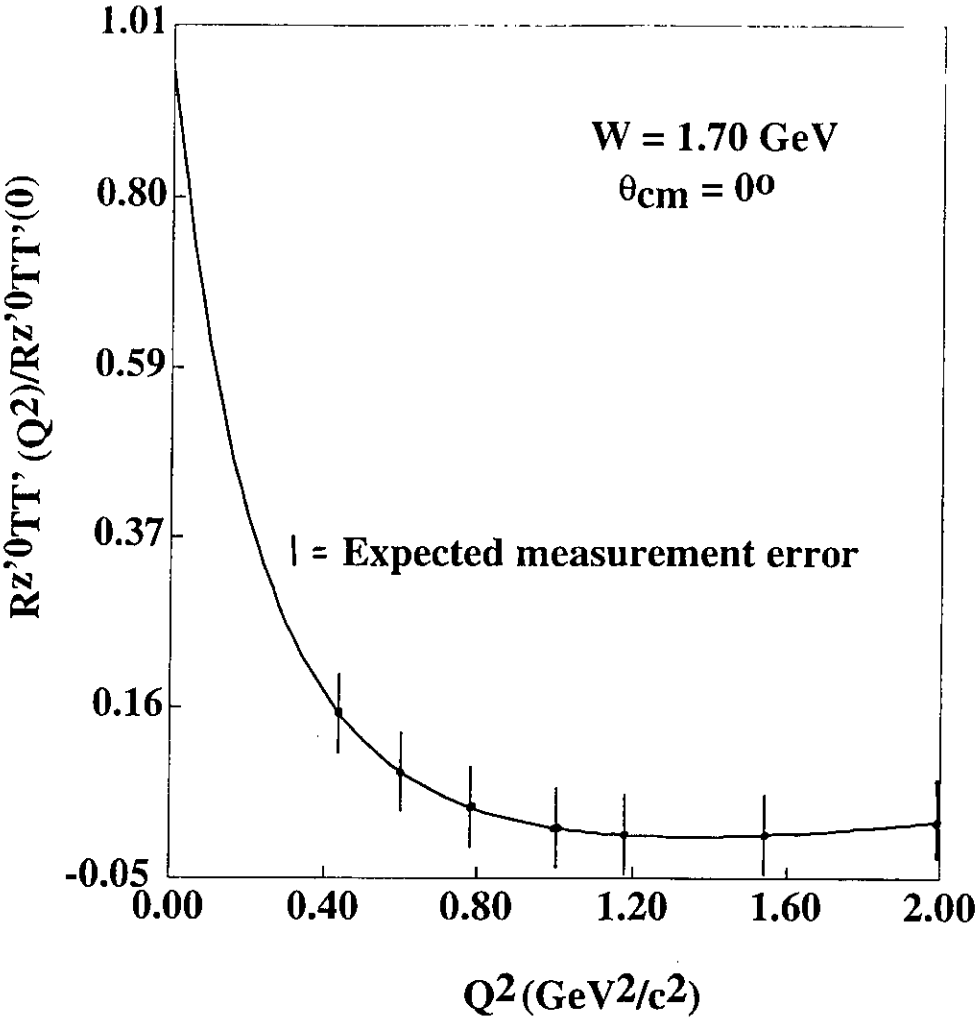

Figure (6). The Q^2 dependence of the the polarization transfer coefficient which will be measured in this experiment. The calculation is by R. Williams. The expected measurement error of the data is shown.

direction of the virtual photon can serve to illuminate the aptitude of the quarks to carry transverse polarization in the hyperon system [21]. The Λ is a uds isosinglet quark system. In the nonrelativistic quark model, if the up and down quark pair form a spin-zero core, the strange quark can carry most of the observed fraction of the spin of the hyperon. A measurement of $R_{TT'}$ over a broad range of Q^2 will yield information on these dynamics.

Other Physics : Fundamental Symmetry Violation

One of the outstanding problems in nuclear and particle physics remains the lack of understanding of the origin of combined charge and spatial (CP) violation (CPV) or, equivalently (if the product of charge, parity and time reversal symmetry (CPT) is valid), time reversal noninvariance (TRNI). So far CPV has been observed only in the weak leptonic decay of neutral kaons [22-25]. The observation in this system is thought to be due to subtle mixing of the neutral kaon and its antiparticle in the production of K^o_L

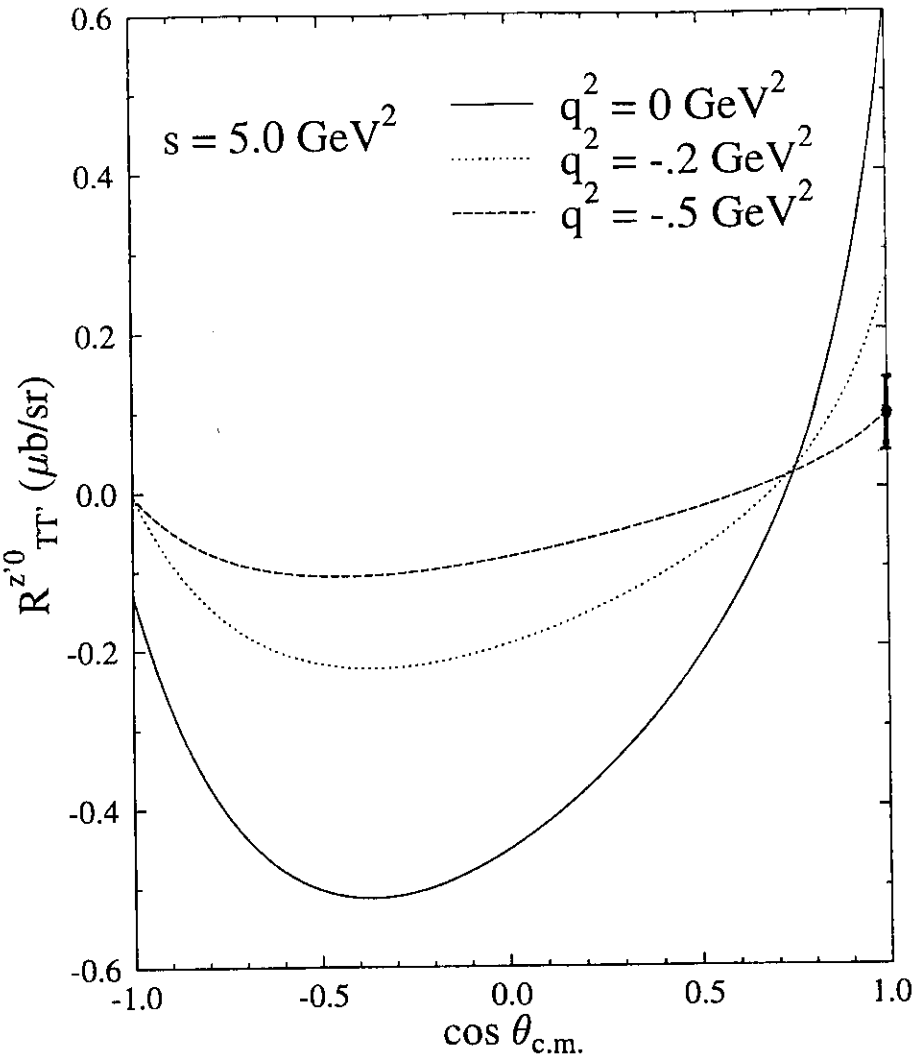

Figure (7). The angular dependence of the polarization transfer response function. The experiment will gather data at the forward angles where the response function is largest. Calculation by R. Williams (1997).

and K^0_S, the long-lived and short-lived, neutral kaons. Hence it is labelled strangeness-changing-two ($\Delta S = 2$) CPV. $\Delta S = 1$, that is to say, direct, CPV has never been observed experimentally, even though it is allowed in the Standard Model of electroweak interactions and in some extensions of the Standard Model [26-29]. Nonleptonic decays of hyperons, in particular, nonleptonic decays of Λ hyperons, is a promising means of searching for direct CPV. The hyperon and kaon in the reaction at CEBAF are produced electromagnetically in such a way that more versatility in controlling their momenta and spin (of the hyperon) is achieved providing complementary information to that from hadron-induced reactions as hyperon production mechanisms [30]. There have been studies which show that even though electromagnetic cross sections are more than an order of magnitude smaller than (π^+, K^+) reaction cross sections, for example, this disadvantage is in part compensated for by the greater intensity and higher quality of electron beams.

If the only information available about the hadrons in the reaction is from the kaon, Λ, and the proton, then three quantities are available for forming a triple (scalar) correlation

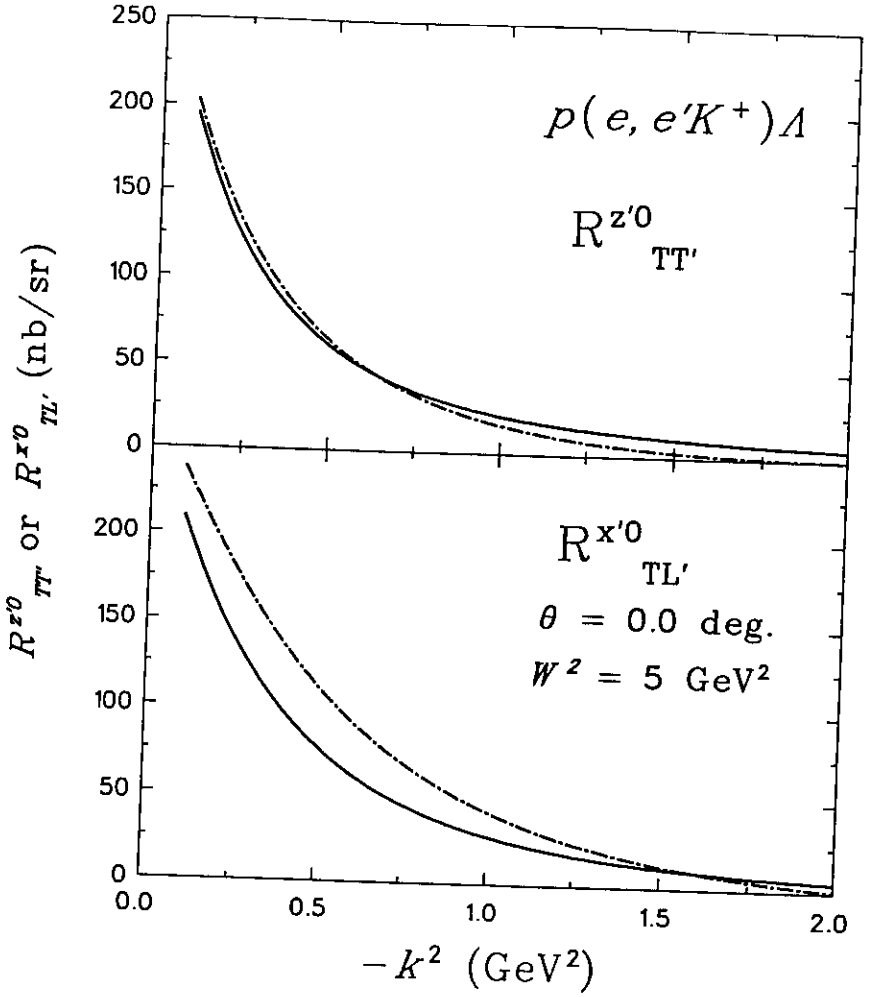

Figure (8). The polarization transfer response function sensitivity to the hyperon form factor versus squared momentum transfer. The curves show that lower momentum transfer is favored for extracting the hyperon form factor. Two different values of the form factor are input which yield the two curves for $R_{TT'}$ in the top figure and $R_{LT'}$ in the bottom figure. Calculation by C. Benhold and T. Mart (1997).

necessary for CPV searches:

$$\vec{\sigma}_\Lambda^{\,\text{induced}},\ \vec{\sigma}_\Lambda^{\,\text{transfer}},\ \vec{\sigma}_\Lambda^{\,\text{interference}} \tag{P3}$$

where $\vec{\sigma}_\Lambda^{\,\text{transfer}}(\vec{\sigma}_\Lambda^{\,\text{t}})$ is the transferred polarization, $\vec{\sigma}_\Lambda^{\,\text{induced}}(\vec{\sigma}_\Lambda^{\,\text{i}})$ is the induced spin polarization, and $\vec{\sigma}_\Lambda^{\,\text{interference}}(\vec{\sigma}_\Lambda^{\,\text{n}})$ is the hyperon spin vector component brought about by the interference between the polarization transfer and induced polarization mechanisms. This interference process has never been searched for previously.

From these vectors, assuming they are independent, the scalar triple correlation product (or some appropriate permutation) may be formed:

$$\vec{\sigma}_\Lambda^{\,\text{t}} \cdot (\vec{\sigma}_\Lambda^{\,\text{i}} \times \vec{\sigma}_\Lambda^{\,\text{n}}) \sim \lambda \tag{P4}$$

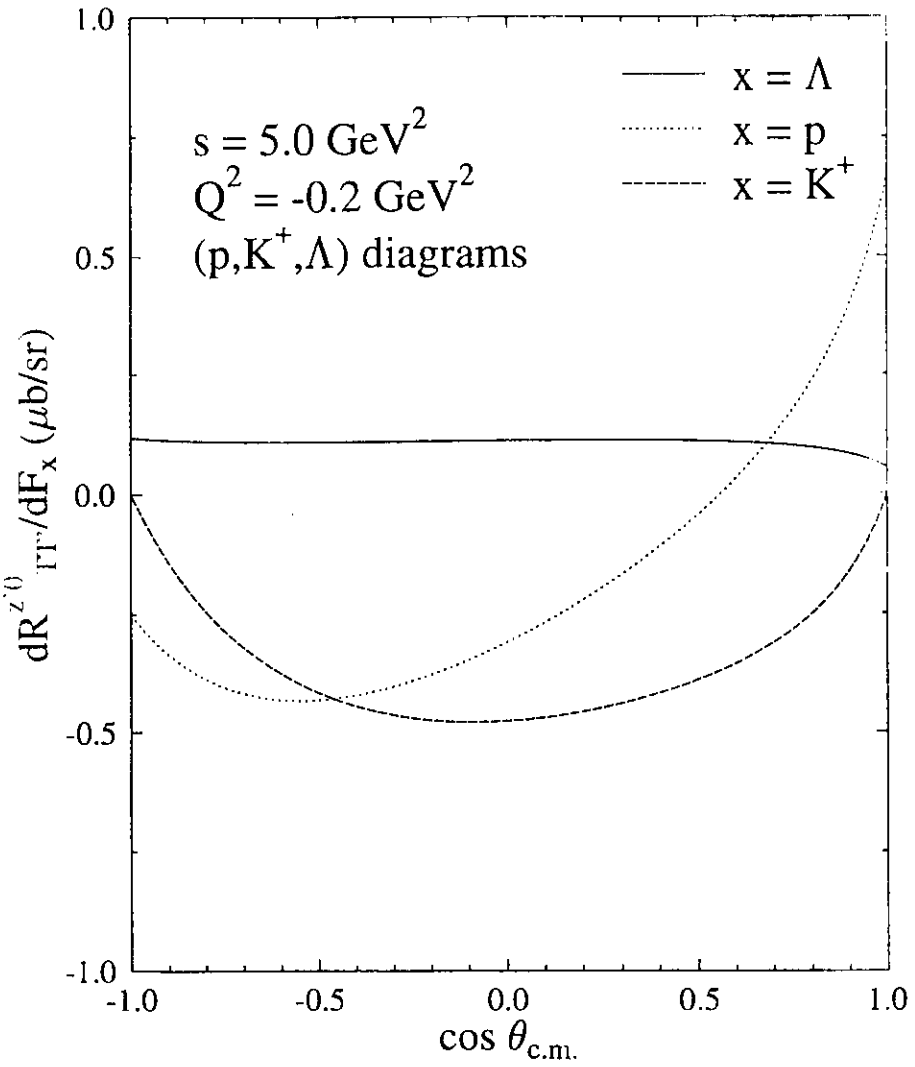

Figure (9). Sensitivity of $R^{z'0}_{TT'}$ to the meson and hyperon form factors versus the production angle. It is seen to be most sensitive in the forward direction. Calculation by R. Williams (1997).

Each of these factors changes sign under the action of the motion reversal and may, in principle, be used to measure the violation of time reversal symmetry as shown later. Thus the triple scalar product (P4) is T-odd, and CP odd [31-33]. One can interpret the correlation product (P4) to mean that the transferred polarization vector cannot have a net component parallel to the direction formed by the cross product of the hyperon induced polarization vector and the hyperon interference polarization vector (if it exists). A term (P4) can arise through interference between induced and transferred polarization in the presence of an N* resonance for example.

There have been several searches for a term in the hyperon decay which is T-odd [34-37]. That such searches are possible may be understood as follows. A quantum mechanical system, unstable with respect to dissociation into two or more particles, decays according to $e^{-\Gamma t}$, the radioactive decay law. This applies to decays owing to the weak interaction. This decay rate, Γ, has in it phases which may give rise to time reversal noninvariance [33]. The phase may be written as

$$\lambda/\alpha = \tan(\Delta\delta + \eta) \tag{P5}$$

where $\Delta\delta$ is the p-π (the hyperon decay products) scattering phase shift arising from the final state (coulomb and strong) interactions between the pion and nucleon. η is the TRNI phase whose nonzero value signals CPV.

A measurement of the partial decay rate, $\Gamma(k)$, of the polarized Λ versus $\vec{k}$ makes possible a determination of the helicity parameter α which measures parity violation in the decay;

$$\Gamma(k) \;=\; \Gamma_0[1 + \alpha(\vec{\sigma}_\Lambda \cdot \vec{k}_p)]. \tag{P6}$$

A measurement of a (net) final state polarization normal to the plane formed by the vectors $\vec{\sigma}_\Lambda^i$ and $\vec{\sigma}_\Lambda^t$ yields λ. Hence a value for $\tan(\Delta\delta + \eta)$ may be found by means of equation (P5).

The phase shift $\Delta\delta$ represents the most intransigent limit to determining a TRNI signature (i.e. to a determination of λ) in Λ decay. It is necessary, therefore, to measure or calculate accurately the strong interaction phase shifts in order to set reasonable limits on the TRNI term in the decay. Final state interactions are unavoidable in any decay experiment. They must be measured or calculated precisely, with that precision being the ultimate limit on the CPV term.

It should be emphasized that the high precision necessary for performing this measurement makes it very arduous, and there is little theoretical guidance on how large the effect might be. Additionally, strong interactions experiments necessary for understanding final state interactions in this decay experiment usually involve interactions between many different channels. Extracting these phase shifts has therefore been difficult. Much progress has been made, however, over the past decade [38-39]. It is now reasonable to claim knowledge of the relevant phase shifts to the level of 0.1°. However, the improved values of the proton-pion phase shifts, the quality of the facility available to perform the measurement, and the fact that the search for such a term has never been attempted before are deemed sufficient motivation for performing the experiment. Statistical accuracy of $\sim 10^{-3}$ are also feasible at CEBAF. This will be the first measurement of the magnitude of such a term in hyperon decay.

In addition to measurement of the λ parameter discussed previously, there are other ways to search for CPV in general [40-41] and specifically in particle decays such as in decay rate differences between particle and antiparticle [42-48], D meson [49] and Φ meson [50] decay, and hyperon electric dipole moment measurements [51]. A measurement of the term proportional to expression (P4) as a search for other physics has never been attempted in this system previously in the manner described [52].

The parity violation parameter α will be determined in the measurement simultaneously with a search for nonzero η for both induced and transferred polarizations. In the case of polarization transfer, the data taken at zero hyperon angles will be used to determine α for this mechanism since there is no induced polarization in this case. For testing parity violation in the case of induced polarization, an unpolarized electron beam will be used with hyperons at nonzero scattering angle. It is expected that the parity violating

decay will be the same in both mechanisms. The search for interference effects will be done using a polarized beam at larger kaon-photon angles where both induced and transferred polarizations are nonzero.

Experimental Setup and Procedure

The experimental setup uses the HMS and SOS in Hall C, with the SOS employed as a hyperon tagger, in addition to its role as a kaon detector. A polarized electron beam of less than 40 μA current with 40% polarization (or whatever is the maximum electron polarization when the experiment is run) will impinge upon the unpolarized cryogenic hydrogen target. The HMS will detect the scattered electron, while the SOS will be used to identify the electroproduced kaon before its decay in flight as well as the proton from the hyperon decay. The hyperon tagger will be used to determine the hyperon momentum and spin by measuring the momentum of the nucleon from the decay

$$\vec{\Lambda} \rightarrow \ \mathrm{p} \ + \ \pi^{-}. \tag{E1}$$

Once the scattered electron and the electroproduced kaon are detected (in coincidence), the reaction is then kinematically complete; the Λ spin direction and momentum are then fixed. The SOS is then placed in the appropriate position (angle and momentum settings) to detect the nucleon from the decay reaction (E1). In the rest frame of the hyperon, the proton and pion emerge back-to-back. The proton momentum vector is constrained to lie in the general direction of the Λ spin vector (the Λ is "self-analyzing"). In the laboratory frame, both nucleon and pion from the decay are detected in the forward direction (at these hadron momenta). Consequently, there is no need to detect the pion in the decay reaction. The decay protons will lie in a rather narrow cone about the direction of the electroproduced hyperon. The size of the cone, and therefore the dimensions of the hyperon tagger, is dictated by the Λ momentum. The Λ spin direction is determined by the angular distribution of the protons using the expression (in the hyperon center of mass frame)

$$\frac{\mathrm{dN}}{\mathrm{d}\Omega_{\mathrm{p}}} \sim (1 + \alpha \mathrm{P}_{\Lambda} \vec{\mathrm{k}}_{\Lambda} \cdot \vec{\mathrm{k}}_{\mathrm{P}}) = (1 + \alpha \mathrm{P}_{\Lambda} \mathrm{k}_{\Lambda} \mathrm{k}_{\mathrm{P}} \mathrm{cos}\phi) \tag{E2}$$

where k is the particle momentum, and ϕ is the angle between the hyperon momentum vector and the proton momentum vector. α is the correlation coefficient (experimentally determined to be 0.642 ± 0.013 [57]) and P_{Λ} is the hyperon spin polarization value. The angle ϕ will be measured with an accuracy of better than 2 mr while the momenta k_{Λ} and k_{p} will be determined with an accuracy of 10^{-3}. (Both angular and momentum accuracy are needed to precisely determine the hyperon decay proton angular distribution in equation (E2)). This level of precision was achieved in the previous Hall C kaon electroproduction experiments (E91-016 and E93-018).

The $\vec{\Lambda}$ spin is flipped by flipping the electron polarization. A schematic diagram of the experimental setup is shown in Fig. (10) and the SOS used as a hyperon tagger is shown diagrammatically in Fig. (11). The experiment will measure N_{a} and N_{p} in order to extract equation (O7) as well as the asymmetry

$$\mathrm{W}(\mathrm{P}_{\Lambda}) = \frac{\mathrm{N}_{\mathrm{p}} - \mathrm{N}_{\mathrm{a}}}{\mathrm{N}_{\mathrm{p}} + \mathrm{N}_{\mathrm{a}}} \tag{E3}$$

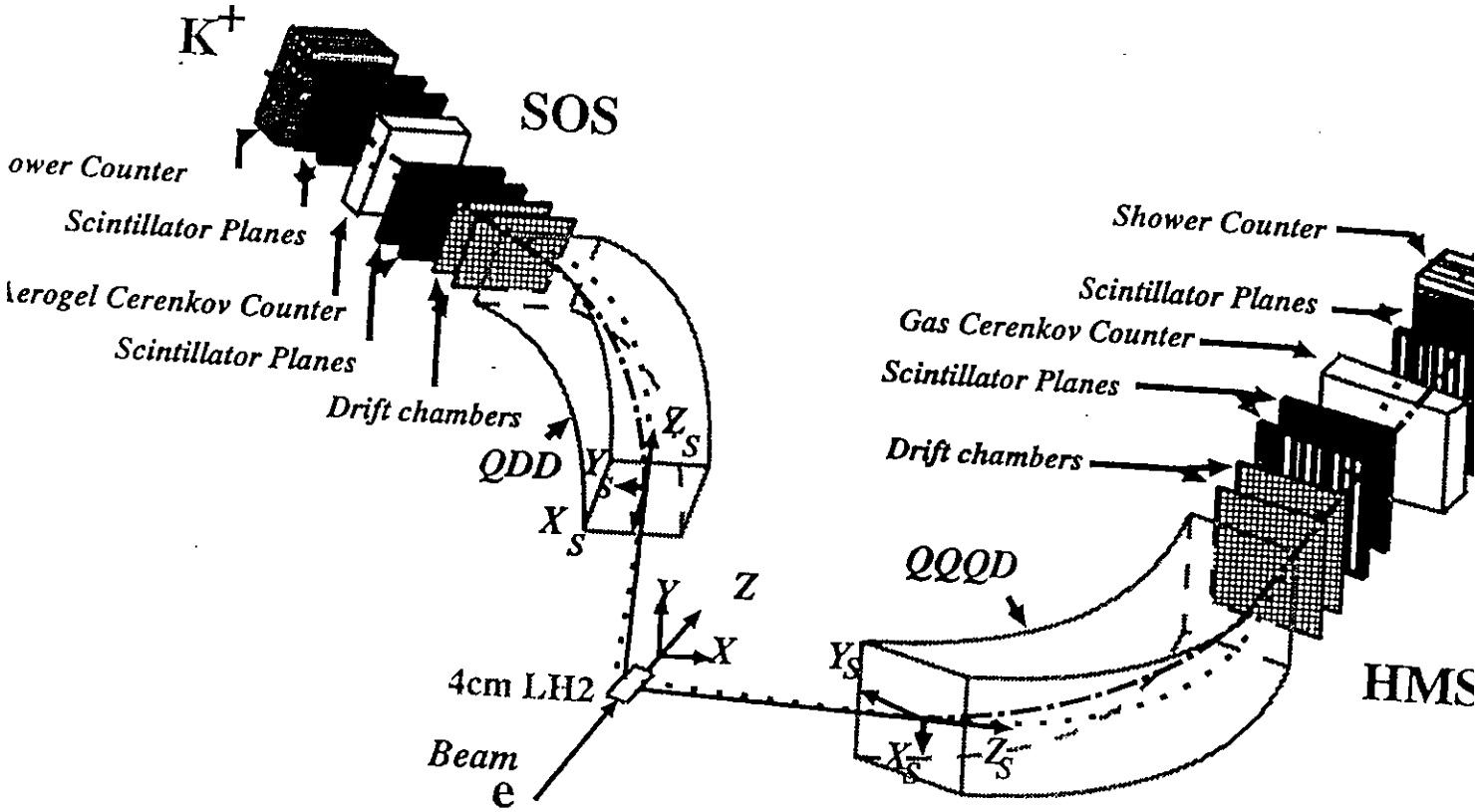

Figure (10). The experimental setup in Hall C. The HMS and SOS will be used to detect the scattered electron and electroproduced hyperon, while, additionally, the SOS will detect the proton from the hyperon weak decay.

where P_Λ is the Λ polarization. N_p (N_a) is the number of coincident electron - kaon - proton events for $\vec{\Lambda}$ spin direction parallel (antiparallel) to the the momentum transfer direction, $\vec{q}$.

The asymmetry $W(P) = \frac{\Delta N}{2N}$ is estimated to be 0.1 for $N \sim 10^5$ counts (see discussion in previous section). Here N is the total number of coincidences detected in the experiment. As shown later in this document, it is not unreasonable to expect $\geq 10^5$ counts in a 12 day run. Then a fractional uncertainty of about 0.3% is measured for W(P). It should be emphasized that this particular measurement has never been attempted before in this manner, and it is most feasible at CEBAF because of the control of the Λ momentum and spin direction. In the case of the $R_{TT'}$ and $R_{LT'}$ measurement, a statistical accuracy at

each data point of $\sim 2\%$ is predicted, on average.

Q^2	E_{in}	E_{out}	Θ_e	Θ_γ	ν	p_γ	W	ϵ
0.455	4.045	2.800	11.500	23.220	1.245	1.416	1.662	0.918
0.604	4.045	2.700	13.500	23.941	1.345	1.553	1.674	0.899
0.765	4.045	2.600	15.500	24.290	1.445	1.689	1.681	0.879
0.990	4.045	2.500	18.000	24.860	1.545	1.838	1.670	0.854
1.171	4.045	2.400	20.000	24.638	1.645	1.969	1.672	0.829
1.539	4.045	2.200	24.000	23.734	1.845	2.223	1.674	0.775
2.059	4.045	1.900	30.000	21.599	2.145	2.581	1.687	0.683

The kinematic parameters are listed in the tables above and below. The incident electron energy is fixed at 4.045 GeV. At each Q^2 point, the hadron spectrometer (the SOS) will be fixed in angle along the virtual photon direction for the extraction of $R_{TT'}$ (where the induced polarization is zero), and for small nonzero angles with respect to the virtual photon when nonzero induced polarization is desired.

Q^2	$P^{SOS}_{central}(=P_{K+})$	$P_\Lambda(\approx P_p)$	$\Theta_{\gamma\Lambda}$	time (days)
0.455	0.704	0.712	0.00	1.5
0.604	0.790	0.763	0.00	1.5
0.765	0.866	0.823	0.00	1.5
0.990	0.898	0.940	0.00	1.5
1.171	0.960	1.011	0.00	2.0
1.539	1.072	1.151	0.00	2.0
2.059	1.267	1.314	0.00	2.0

The HMS Detector and Background Estimates

The choice of electron momentum and angle for the experiment is dictated by several considerations:

(i) The electroproduction cross section is a moderately strong function of the virtual photon momentum in this region. Large kaon (and therefore Λ) count rates are needed.

(ii) Sufficient photon momenta are necessary so that the emergent kaons have enough momenta that a large fraction are detected before decay in the SOS.

(iii) The minimum HMS angle. Small angles are favored, in some cases.

The HMS will be used in the point to point tune mode (the same as was used in E93-018). The quadrupole magnets serve to focus the scattered electrons, and therefore define

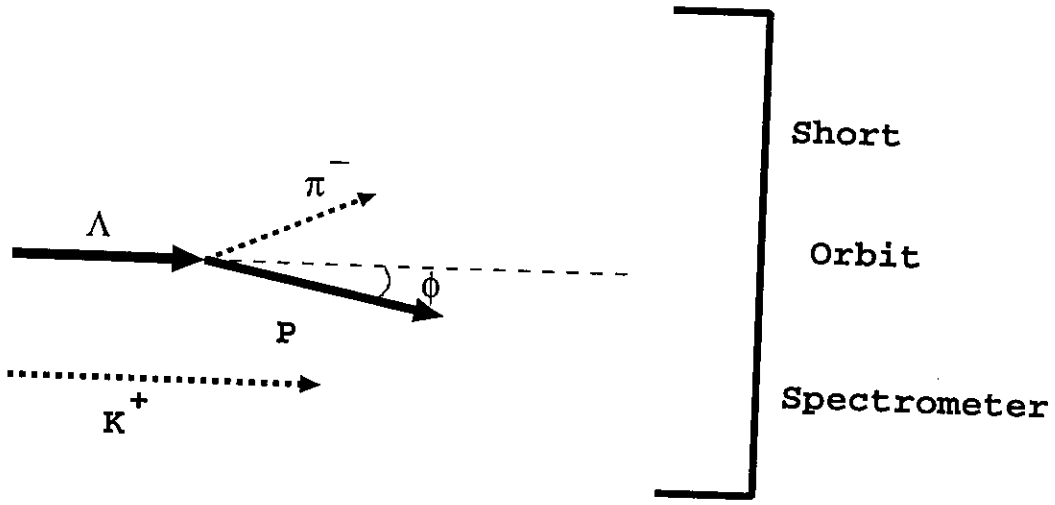

Figure (11). The SOS used as a hyperon tagger. The decay protons from the reaction (O4) are detected in the SOS spectrometer, thus tagging the hyperon spin polarization vector.

the experimental solid angle, while the momentum determination is achieved by bending these same electrons in the dipole magnet. The largest contribution to the reconstructed electron momentum accuracy in the HMS resolution is $\frac{\Delta p}{p} \leq 10^{-3}$.

The detector stack for the HMS detector is shown in Fig. (10). The detector stack uses standard focal plane instrumentation and is the same configuration used in E93-018. There will be drift chambers for charged particle tracking, a gas Cherenkov detector for particle identification, scintillator hodoscopes for fast timing, and Pb-glass shower counters for calorimetry.

Charged particle trajectories will be measured using 2 multiwire drift chambers each having XYUVY′X′ planes with the U and V stereo planes at 15° with respect to the X and X′ planes. The X′(Y′) planes are offset by 1/2 cell from the X(Y) planes. Thus there will be 12 multiwire planes before the scintillator hodoscopes or Cherenkov detector. The drift chambers will have cell sizes of 10 mm × 8 mm. Initial experiments which make use of the HMS drift chambers have shown that spatial resolutions of better than 170 μm (σ) can be expected up to the highest rates that will be encountered in the experiments using the HMS.

The scintillator hodoscopes will be used for fast timing while the shower counters

will be used for charged particle energy determination. The gas Cherenkov detector will be used for π-e and p-e discrimination. Additionally, there should be some separation of charged particles from the Pb:glass shower counters. It has been demonstrated that pion-electron separations of 500/1 will be sufficient to reduce the backgrounds to acceptable levels.

The SOS Detector and Background Estimates

Kaon Kinematics

The choice of kaon momenta in the $p(\gamma_v, K^+)Y$ reaction is dictated by:

(i) The hyperon recoil momentum. A moderately large hyperon recoil momentum is needed so that the decay products are focussed in a rather small cone in the direction of the hyperon momentum.

(ii) The limits of the SOS spectrometer angles and momenta.

(iii) Matching the kaon and hyperon momenta.

The kaon (SOS) spectrometer will use standard focal plane instrumentation as shown in Fig. (10). There will be two sets of drift chambers (a total of 12 planes), measuring positions along X, Y, and U and V (stereo angles). Scintillator hodoscopes (four planes) will be used for fast timing.

The SOS is a focusing spectrometer with a very short flight path (compared to the HMS). This short flight path enhances the detection of the short-lived kaons before their decay in flight.

The proposed SOS detector package consists of two sets of planar drift chambers, scintillator hodoscopes, followed by a second array of scintillators, and an Aerogel Cherenkov counter. It is advantageous, in the SOS, to use the time-of-flight differences between protons, pions, and kaons to identify these charged particles (and therefore to separate them). By maximizing the distance between the S1 and S3 scintillator arrays in the SOS detector hut, charged particle separation has been easily achieved.

The proton-kaon time difference is large enough at all momenta that the time difference may be resolved. For the higher momentum settings, judicious use of the Aerogel Cherenkov counter and some time-of-flight separation may be used to yield a clean kaon signal. It has been demonstrated in previous Hall C experiments that using this system, a pion rejection (the most insidious problem) of approximately 10^3 is achievable. This rejection ratio has been demonstrated in E93-018 to be adequate for this experiment [53].

The momentum of a charged particle will be determined by reconstructing its trajectory through the dipole (bending) magnet while the production angles are then obtained by tracing the trajectory through the quadrupole (focusing) magnets back to the target position. The maximum momentum acceptance is 20% (40%) while the solid angle is approximately 5 msr for the HMS (SOS) spectrometer using the point to point tune. This technique will be used for both arms of the experiment.

The SOS As A Hyperon Tagger

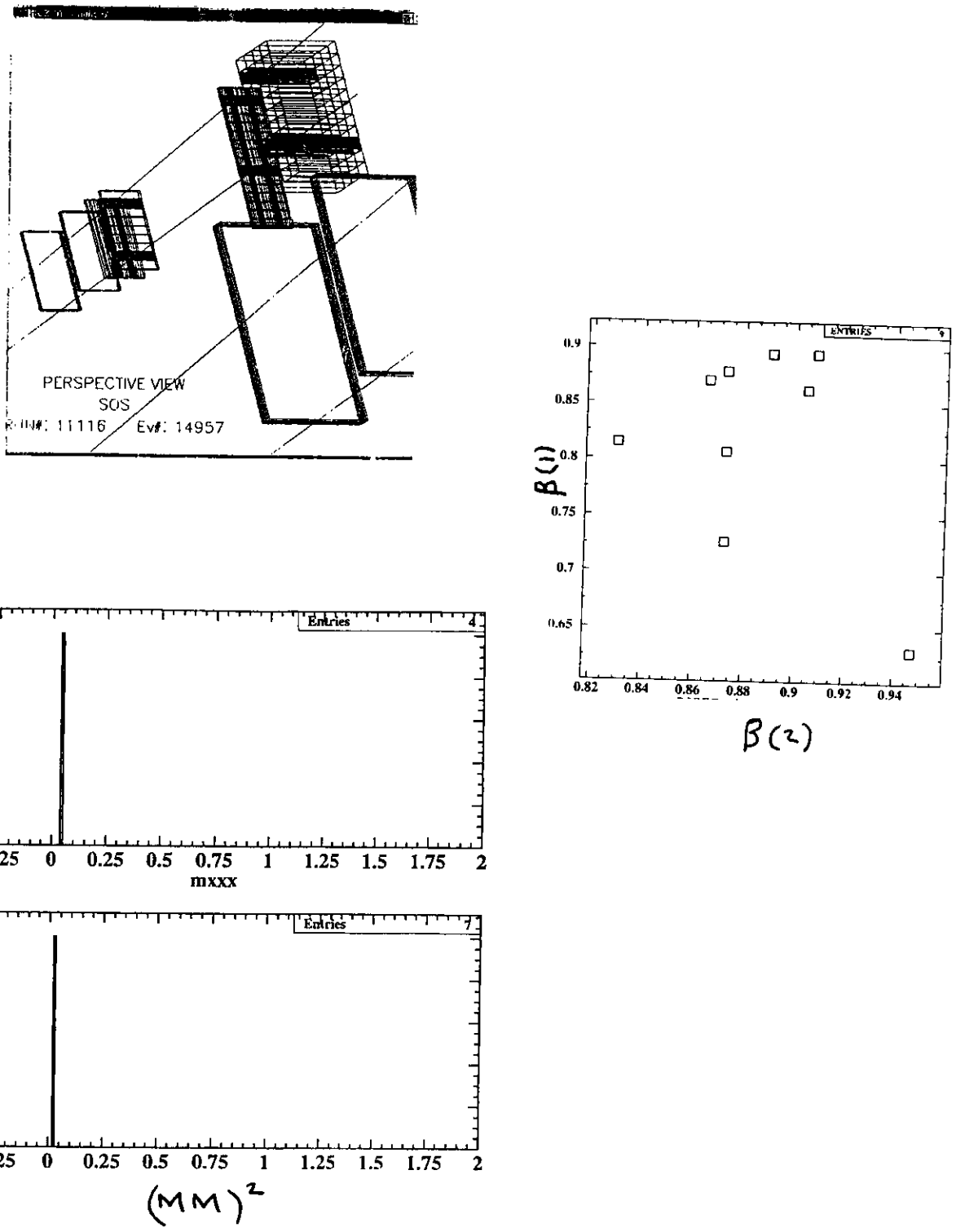

Figure (12). The single event display of an event in SOS detector stack with two particle tracks (top). Particle identification is determined from the particle velocity (middle). The calculated missing mass is used to determine that this is the reaction given by equation (E4). The SOS will be used to identify kaons as well as protons in the same event.

The SOS will be used as a hyperon tagger by detecting the decay proton from the

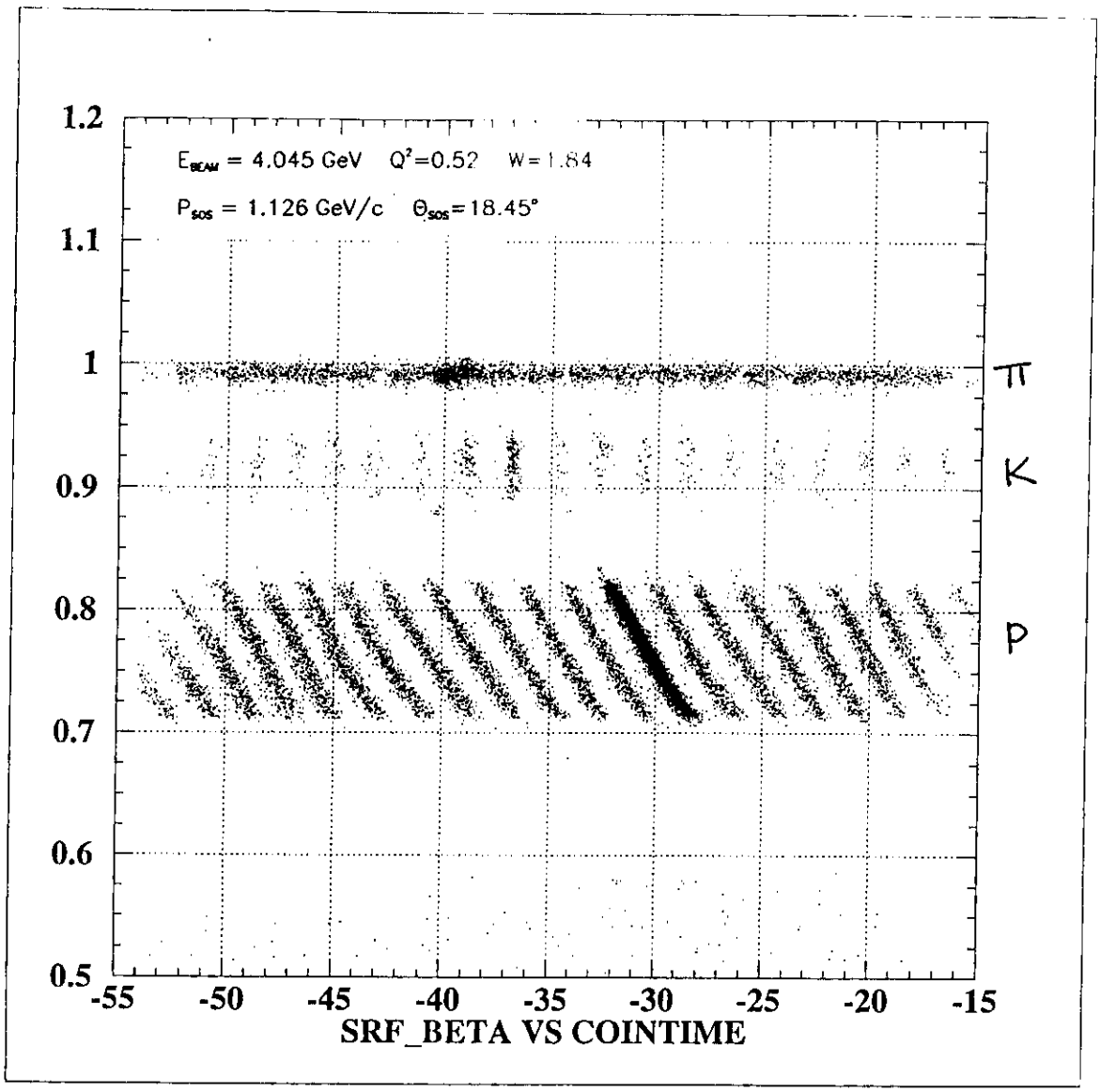

Figure (13). Data taken during E93-018 showing time of flight differences for a 1.0 GeV/c momentum setting in the SOS with positive polarity. This data was taken in one hour with 30 μA of beam.

reaction (O4). Only the decay proton momentum vector needs to be determined, not its spin vector. Both timing (TDC) and pulse height (ADC) information will be gathered at each end of the separate scintillator bars. The SOS has already been used to serve this purpose in the previous kaon electroproduction experiments. The technique described here for detecting the kaon and decay proton in the same event is shown in Fig. (12) for one event. This figure is meant to demonstrate that the proposed technique works, and that the analysis of the data as proposed is justified.

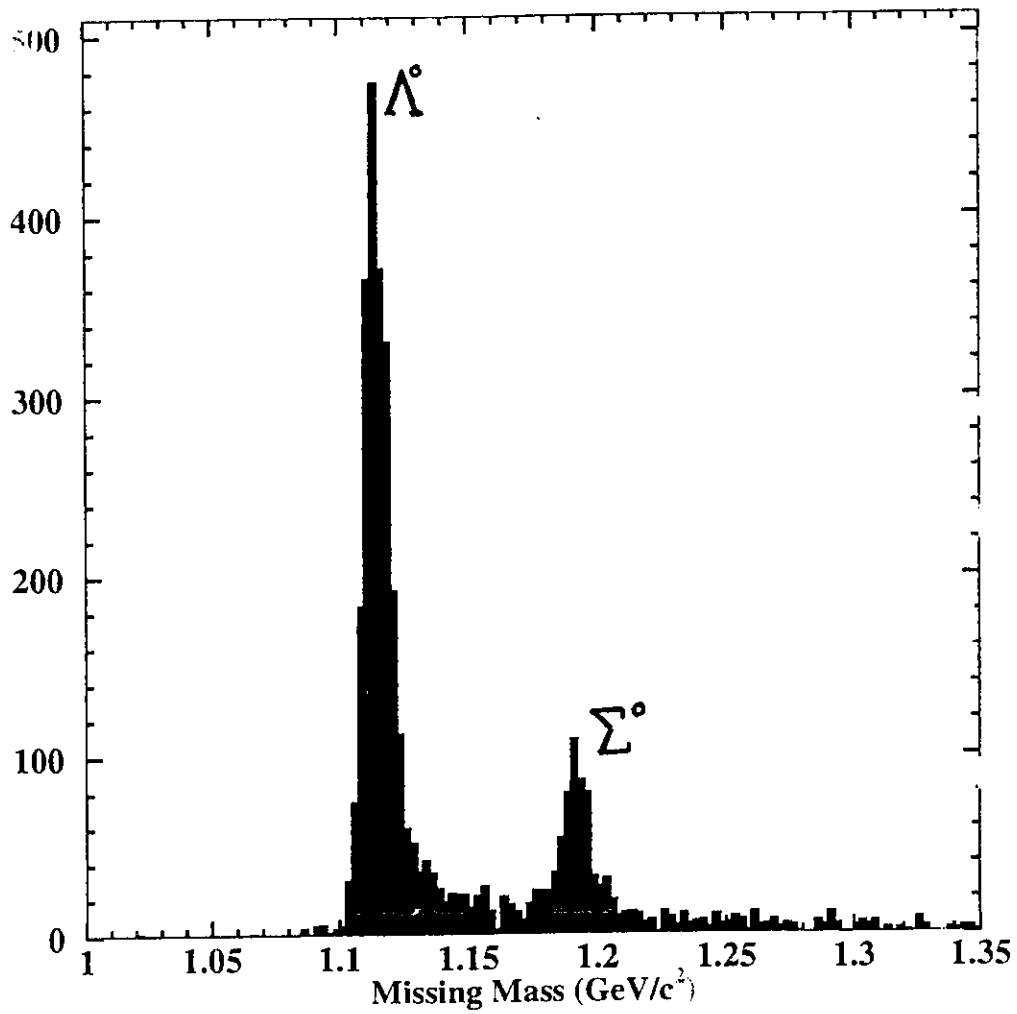

Figure (14). Data taken during E93-018 showing the hyperons identified in the missing mass spectrum of the reactions (P1) and (P2). The data was taken in less than one hour with 30 μA of beam.

The procedure proposed for data analysis has been tested on a subset of the data from E93-018, recently completed in Hall C. For one series of measurements at, the kaons and hyperons were both produced at forward angles (in the laboratory system) with respect to $\vec{q}$ and with the same laboratory momenta. The scattered electrons were detected in the HMS while the kaons were detected in the SOS before their decay in flight. The particle

identification for the reaction shows clearly the kaons from the reaction in Fig. (13). For these momenta, a clear Λ peak in the missing mass spectrum is seen (see Fig. (14)). In some fraction of these coincident events, a second particle with the velocity identified with that of a proton, was detected in the SOS, in coincidence with the kaon. From the measured energy and momentum of the scattered electron, kaon, and coincident proton, a missing mass (mass of X) of the process

$$e + p \rightarrow e' + K^+ + p + X \tag{E4}$$

was determined, indicating that the particle was a pion from the decay

$$\Lambda \rightarrow p + \pi^-. \tag{E5}$$

The single event display for the SOS detector stack is shown in Fig. (12) for an event where two particle were detected within the same coincidence window. For this event, the beta of particle 1 (2) is 0.83 (0.64). From the SOS momentum setting the particle is identified as a kaon (proton). The pion in the corresponding missing mass calculation indicates that the analysis procedure works. Hence, this analysis procedure can be used to identify the Λ decay products from the kaon electroproduction event (the hyperons are determined from missing mass in the standard way). This technique will be applied for all of the kinematic points measured in this experiment.

The effect of the finite SOS (polar) angular acceptance is shown in Fig. (15). Plotted is the Λ-hyperon angle with respect to the virtual photon, in both the lab frame and the center of mass frame, versus the kaon - photon lab angle. The SOS angular acceptance is about 5 degrees corresponding to a maximum hyperon - photon angle of just under 30° in the center of mass. The kaon and hyperon momenta in the experiment for a representative set of kinematics is shown in Fig. (16) for the finite HMS (electron arm) acceptance. Again, the kaon and hyperon momenta must be roughly equal in order for the SOS to be used as a hyperon tagger in the manner proposed. The rather large momentum acceptance in the SOS as indicated in the figure, permits kaons and protons from hyperon decay to be detected over a large momentum range.

The Hydrogen Target and Electron Beam

The (unpolarized) hydrogen target planned for the experiment will be 4.0 cm in length and 6.4 cm in diameter. This target container, cylindrical in shape, will have 0.08 mm thick aluminum end-windows. The effective length as 'seen' by each spectrometer is calculated based upon Monte Carlo simulation.

The uncertainty in the length of the target and target density is expected to be about 1 per cent. For the density, the calculated value based upon 19.0° K temperature and 16 psi pressure (operating parameters) is 0.070 g/cm^3. For each point, a target empty and a target full run will be made.

The experiment will use a longitudinally polarized electron beam with a maximum current of 40 μA and 40% polarization (or whatever is the maximum polarization available

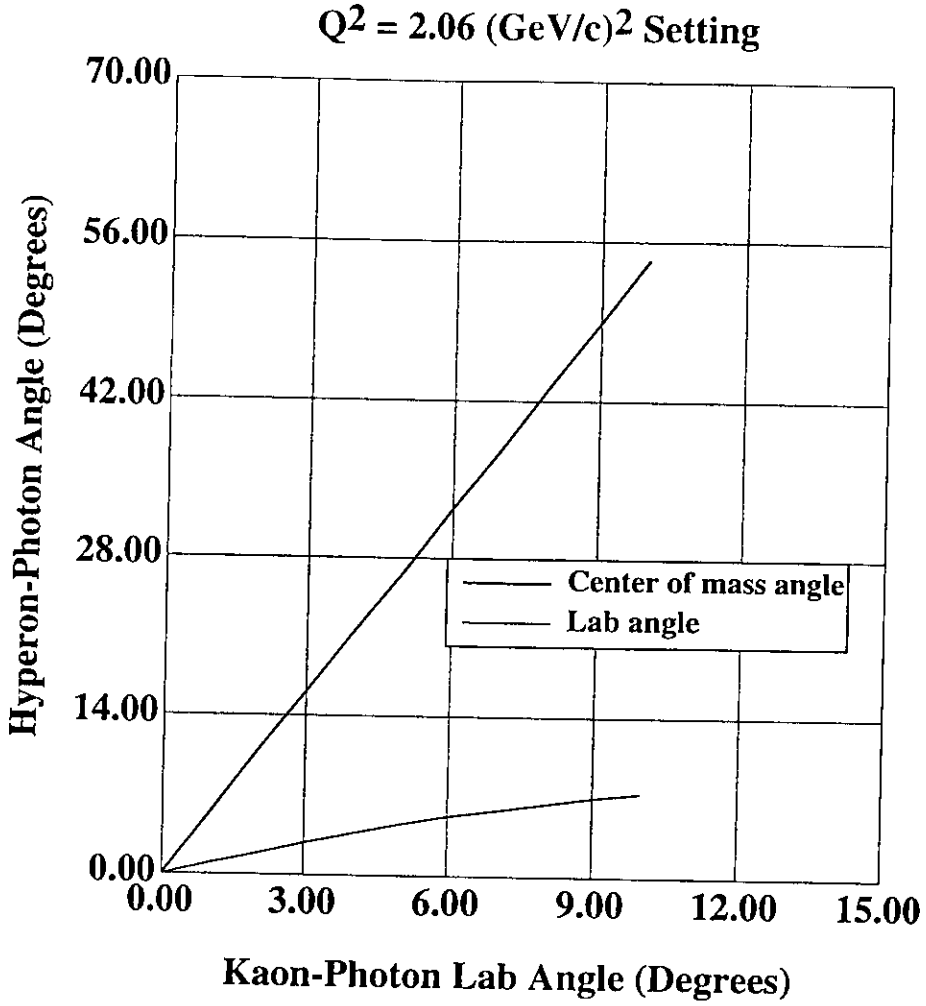

Figure (15). The angular acceptance in the SOS for hyperons with respect to the virtual photon versus kaon - photon lab angle. The SOS has roughly a 5 degree full angular acceptance.

at the time of the experiment). The beam current will be measured using the standard beam current monitors in Hall C. The beam polarization will be measured using the Mott polarimeter which is currently being used in polarization measurements.

Electronics and Trigger

The experiment will use the CEBAF On Line Data Acquisition system (CODA) developed at CEBAF. The trigger in the HMS detector will consist of scintillator and Cherenkov hits to separate out electrons from pions and kaons (mainly) and antiprotons. Symbolically, the HMS trigger will be

$$S_1 \cdot S_2 \cdot C_e \cdot Sh \qquad \text{(E6)}$$

where S_1 (S_2) is the first (second) XY pair of scintillator hodoscopes, C_e is the gaseous Cherenkov detector which will fire on electrons and not pions or kaons, and Sh is the HMS shower counter. Time-of-flight separation will be adequate for e-K^- separation at

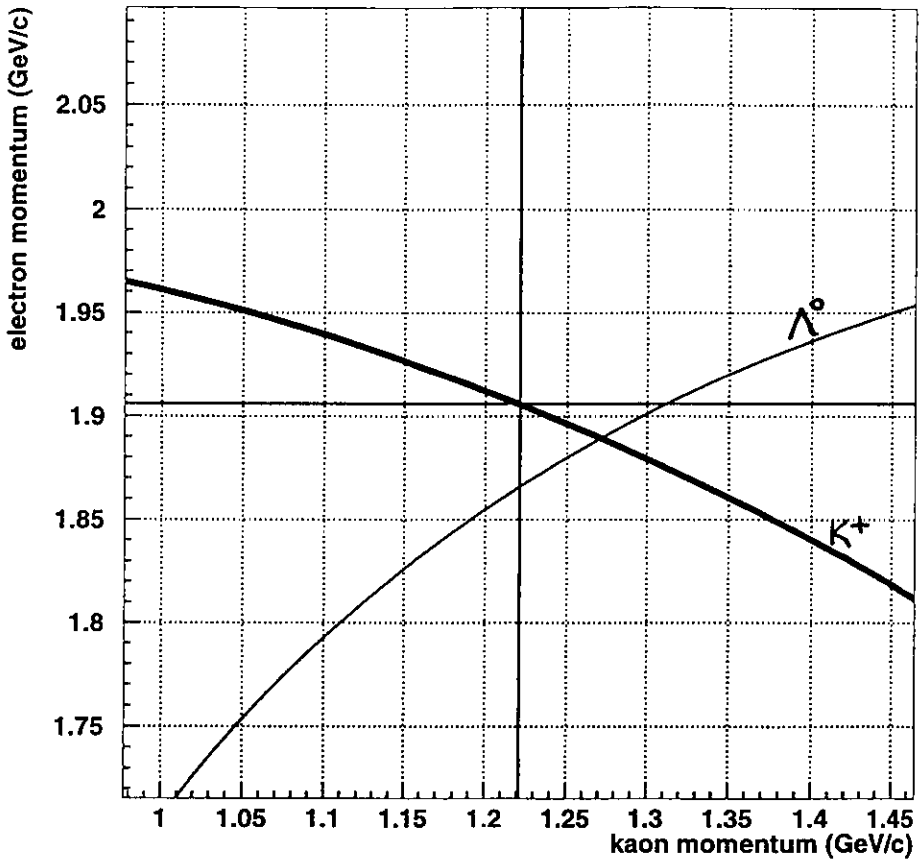

Figure (16). The momentum range in both the SOS and HMS for a representative kinematic setting of the experiment. The large SOS momentum acceptance gives flexibility in detecting both the kaon and the proton from the hyperon decay.

all momentum in the experiment for the HMS. The SOS will use a trigger to separate out kaons from pions, positrons, and protons mainly. Symbolically, the hadron arm trigger will be

$$S_1 \cdot S_2 \tag{E7}$$

where, again, S_1 (S_2) is the first (second) XY pair of scintillator hodoscopes. Time of flight separation is achievable at all momentum settings in this experiment.

Expected Corrections

Previous work in p(e,e'K^+) experiments indicate that the detector stack will give uncertainties associated with each detector element as corrections are applied to the detectors. The corrections will be determined by Monte Carlo simulations and during the

actual experiment. The expected uncertainties associated with the corrections are listed as follows.

Counter Dead Time	2 %
Wire Chamber Inefficiencies	0.5 %
Electron Shower Counter Inefficiencies	1 %
Kaon Absorption in target/detectors	1 %
Kaon Arm Cherenkov-Counter Inefficiencies	2 %
Kaon Decay	3 %
Knock-on Events Firing Cherenkov	1 %
Target Wall Events	1 %
Randoms	1 %
In Time Kaon Losses	1 %
Radiative Corrections (Photon Radiations)	3 %
Beam Polarization (40% polarization)	1 %
Quadratic Sum	$\pm$ 5 %

Note that this is 5 % of the corrections which are expected to be about 30 - 70%. The total systematic uncertainty due to the above corrections is expected to be about 3.5%.

The asymmetry in the polarization transfer measurement (O3) will be determined to better than 5%. Then the polarization transfer coefficient $R_{TT'}$ will be determined (from equation (O8)) to better than 5%.

Monte Carlo Simulation

A Monte Carlo simulation package has been developed which provides a good model of the Hall C setup to be used in this series of measurements. The software package was originally developed and used for a set of (e,e'p) experiments at SLAC [54] and later adapted to the Hall C configuration for use in the (e,e'K) experiments [55]. The Monte Carlo randomly generates the target quantities $(p_{e'}, \theta_{e'}, \phi_{e'})$ and (p_K, θ_K, ϕ_K) for the scattered electron and electroproduced kaon, respectively. The measured HMS and SOS angular and momentum acceptances are used. The energy and position of the incident electron beam at the target were randomly generated and matched to the energy spread and spatial extent of the CEBAF beam (as observed in the recently completed kaon electroproduction experiments). The scattered electron and electroproduced kaon were then transported through single arm Monte Carlo models of the HMS and SOS. Realistic scattering from various materials in the spectrometer, ionization losses, and multiple scattering are included. For the hadron arm (the SOS), charged particle decays (such as kaon decays) are incorporated where appropriate. The reconstruction package used in the extraction of experimental quantities from the data (COSY) is employed to generate the MC results.

The reaction (O3), once the proton from Λ decay is detected, is kinematically complete; the pion from reaction (O4) can be determined from the missing mass spectrum. The ratio of integrated events under the peaks of the kaon and pion in the missing mass spectra give an estimate of the number of protons from Λ decay that can be expected in the experiment. (The proton in this case is used to identify the Λ spin polarization vector.) The results of the monte carlo indicate that on average, about 6% of the kaons (for unpolarized Λ hyperons) which give reconstructed Λ-hyperons yield an identified π^- meson. These results were first obtained by B. Mecking using a separate Monte Carlo simulation with measured HMS and SOS acceptances [56]. This results was used in estimating the required measurement time for each data point.

Rates And Beam Time Request

The singles rates, R, in each of the spectrometers separately was obtained from the results of experiment E93-018 which are consistent with

$$R = n_i \cdot n_t \cdot t \cdot \frac{d\sigma}{d\Omega} \cdot \Delta\Omega \cdot (1 - P_{decay}) \tag{E8}$$

where n_i is the number of incident particles per second on a target of thickness t and target density n_t. $d\sigma/d\Omega$ is the scattering cross section and $\Delta\Omega$ is the spectrometer solid angle. The count rate is corrected for kaon survival probability.

In the electron arm, the singles rates were measured to be below 10 kHz when using a 35 μA beam and the 4-cm target and with the HMS at a forward angle. This is well below the design limit for the detectors in the spectrometer detector stack. In the hadron arm, the singles rates are kept below 1 MHz with 35 μA beam current. Again, this is adequate for the experiment.

The coincidence rate, R_{coinc}, for the HMS and SOS used in this experiment is known from the results of the Hall C kaon electroproduction experiments (using an unpolarized electron beam). The cross section is extracted using the formula:

$$R_{coinc} = \frac{i}{e} \cdot \frac{\rho t N_o}{A} \cdot \epsilon_D \cdot \frac{d^3\sigma}{dE_e d\Omega_e d\Omega_k} \cdot \Delta E_e \Delta\Omega_e \Delta\Omega_k (1 - P_{decay}) \tag{E9}$$

Here $\Delta\Omega$ is the solid angle of the spectrometer, ϵ_D is the detection efficiency, i is the beam current, N_o is Avogadro's number, e is the electron charge, t is the target thickness of mass number A and density ρ. For the HMS spectrometer, $\Delta E/E$ will be about 20%.

An estimate of the number of accidental to true coincidences A/T is obtained from

$$\frac{A}{T} = \frac{\tau R_e R_k}{f\ R_{coinc}} \tag{E10}$$

where the duty factor f is 100% for the CEBAF machine and the resolving time, τ, is taken to be 1.0 ns offline and 30 ns online. Although A/T could be reduced somewhat by lowering the beam current (at the expense of counting rates), this ratio should allow a 2% (statistical) measurement without difficulty. Currently, in the analysis of the E93-018 data, A/T ratios of 1/100 are reasonable offline.

A measurement at the momentum transfers proposed here with the statistics required will require approximately 15.0 days of floor space, including setup time. This is summarized in the table below.

Beam Time Request

	Time (Days)
Data Acquisition	12.0
Setup and Checkout	1.5
Background Studies	1.0
Angle and Momentum Changes	0.5
TOTAL	15.0

The Collaboration

The collaboration will include institutions and personnel that have made substantial contributions to building hardware and readying software for the experiment. Additionally, most of these collaborators will have taken part in the initial kaon electroproduction experiments (E91-016 and E93-018) in Hall C during the fall of 1996. Graduate students will use this experiment as part of their dissertation research. The Hampton University group has 6 graduate students, 3 postdocs and 3 (presently) faculty members involved in experimental work, and 2 faculty, 1 postdoc, and several students providing theoretical support. Other institutions provide similar levels of effort as part of this collaboration.

REFERENCES

1. J. D. Walecka, Argonne National Lab. Report ANL-83-50 (1983).
2. S. Nozawa and T. S.Lee, Nucl. Phys. A513, 511 (1990).
3. W. E. Kleppinger and J. D. Walecka, Ann. Phys. 146, 349 (1983).
4. T. De Forest, Jr., Ann. Phys. 45, 365 (1967).
5. G. Gourdin, IL Nuovo Cim. 221, 1094 (1961).
6. D. R. Yennie et. al., Rev. Mod. Phys. 29, 144 (1957).
7. G. Knochlein et al., Z. Phys A (1996).
8. R.A. Adelseck and B. Saghai, Phys. Rev. **C42**, 108 (1990).
9. H. Genzel et al., *Photoproduction of Elementary Particles*, Group I, V8 of *Landolt-Bornstein, Numerical Data and Functional Relationships in Science and Technology*, Springer Verlag, Berlin (1973).
10. See for example R. K. Bhaduri, **Models of the Nucleon**, Addison-Wesley Publ. Co., Menlo Park, CA (1988).
11. J.M. Finn and P.A. Souder et al., CEBAF PR 91-010.
12. D. Beck et al., CEBAF PR 91-017.
13. L.L. Foldy, Phys. Rev. **83**, 688 (1955).
14. L.L. Foldy, Rev. Mod. Phys. **30**, 471 (1958).
15. R.G. Arnold et al., Phys. Rev. Lett. bf 57, 174 (1986).
16. C. Bennhold, Phys. Rev **C43**, 775 (1991).
17. R. Hofstadter et al., Rev. Mod. Phys. **30**, 482 (1958); R. Hofstadter et al., Phys. Rev. **98**, 217 (1955).
18. NSAC Report (1989).
19. B. Krusche et al., Phys. Rev. Lett (1996).
20. R. W. Williams, Ph. D. Dissertation, NCSU (1993).
21. M. Burdart and R.L. Jaffe, Phys. Rev. Lett. **70**, 2537 (1993); X. Artru and M. Mekhfi, Nucl. Phys. **A532**, 351c (1991).
22. J.L. Ritchie and S.G. Wojicki, Rev. Mod. Phy. **65**, 1149 (1993).
23. B. Winstein and L. Wolfenstein, Rev. Mod. Phy. **65**, 1113 (1993).
24. R.D. Pecci, invited talk , 23rd INS international Symposium on Nuclear and Particle Physics with Meson Beams in 1 GeV/c Region, Tokyo, Japan (1995).
25. L. Wolfenstein, Ann. Rev. Nucl. Part. Sci. **36**, 137 (1986).
26. X-G. He et. al., Phy¿ Let. **B272**, 411 (1991).
27. J.F. Donoghue and S. Pakvasa, Phy. Rev. Lett. **55**, 162 (1985).
28. J.F. Donoghue et. al., Phy. Rev. D **34**, 833 (1986).
29. X-G. He and G. Valencia, Phy. Rev. D **52**, 5257 (1995).
30. O.K. Baker, in **Intersections Between Particle and Nuclear Physics**, ed. by S. Seestrom, AIP Conf. Proc. **338**, 626 (1994).
31. E.M. Henley, Ann. Rev. Nucl. Sci **19**, 367 (1969).
32. E.M. Henley, Fundamental Symmetry Tests With Neutron Beams, ed. by D. Bowman et. al. (1987).
33. R.G. Sachs in **The Physics of Time Reversal**, the Univ. of Chicago Press (1987).
34. O.E. Overseth, Phy. Rev. Lett. **19**, 395 (1967).

35. O.E. Overseth and R.F. Roth, Phy. Rev. Lett. **19**, 391 (1967).
36. W.E. Cleland et. al., Nucl. Phy. **B40**, 221 (1972).
37. W.E. Cleland et. al., Phy. Let. **B26**, 45 (1967).
38. Y. Surya and F. Gross, Preprint WM-95-101 and CEBAF-TH-95-04 (1995).
39. R.A. Arndt et. al., Phy. Rev. C **52**, 2120 (1995).
40. R.I. Steinberg et. al., Phy. Rev. Lett. **33**, 41 (1974).
41. R.M. Baltrusaitis and F.P. Calaprice, Phy. Rev. Lett. **38**, 464 (1977).
42. T. Brown et. al., Phy. Rev. Lett. **51**, 1823 (1983).
43. L-L. Chau and H-Y. Cheng, Phy. Let. **B131**, 202 (1983).
44. M.J. Iqbal and G.A. Miller, Phy. Rev. D **41**, 2817 (1990).
45. J. Antos et. al., Fermilab Proposal P-871 (1994).
46. M. Lu et. al., Phy. Let. **337**, 133 (1994).
47. J.F. Donohue et. al., Phy. Let **B178**, 319 (1986).
48. X-G. He et. al., Phy. Rev. D **47**, R1744 (1993).
49. J. Bartelt et. al., Phy. Rev. D **52**, 4860 (1995).
50. A. Dzierba, Plenary Talk given at CEBAF Upgrade Workshop (1994).
51. L. Pondrom et. al., Phy. Rev. D **23**, 813 (1981).
52. See, however, S.Y. Hsueh et. al., Phy. Rev. D **38**, 2056 (1988).
53. O.K. Baker et al., CEBAF PR93-018 (1993).
54. N. Makins, Ph.D. Dissertation, MIT (1994).
55. P. Gueye, private communications, (1995).
56. B. Mecking, private communications (1996).
57. M.I. Adamovich et al., Z. Phys. **A350**, 379 (1995).
58. C. Benhold and T. Mart, private communications (1997).

HAZARD IDENTIFICATION CHECKLIST

JLab Proposal No.: _____ Date: _____
(For CEBAF User Liaison Office use only.)

Check all items for which there is an anticipated need.

Cryogenics
- _____ beamline magnets
- _____ analysis magnets
- ✓ target
  - type: H2
  - flow rate: Standard
  - capacity: standard

Electrical Equipment N/A
- _____ cryo/electrical devices
- _____ capacitor banks
- _____ high voltage
- _____ exposed equipment

Radioactive/Hazardous Materials
List any radioactive or hazadorous/ toxic materials planned for use:
N/A

Pressure Vessels N/A
- _____ inside diameter
- _____ operating pressure
- _____ window material
- _____ window thickness

Flammable Gas or Liquids N/A
- type: _____
- flow rate: _____
- capacity: _____

Drift Chambers
- type: Ethane
- flow rate: Standard
- capacity: Standard

Other Target Materials N/A
- ___ Beryllium (Be)
- ___ Lithium (Li)
- ___ Mercury (Hg)
- ___ Lead (Pb)
- ___ Tungsten (W)
- ___ Uranium (U)
- ___ Other (list below)

Vacuum Vessels N/A
- _____ inside diameter
- _____ operating pressure
- _____ window material
- _____ window thickness

Radioactive Sources N/A
- _____ permanent installation
- _____ temporary use
- type: _____
- strength: _____

Large Mech. Structure/System
- _____ lifting devices N/A
- _____ motion controllers
- _____ scaffolding or
- _____ elevated platforms

Lasers N/A
- type: _____
- wattage: _____
- class: _____

Installation:
- _____ permanent
- _____ temporary

Use:
- _____ calibration
- _____ alignment

Hazardous Materials N/A
- ___ cyanide plating materials
- ___ scintillation oil (from)
- ___ PCBs
- ___ methane
- ___ TMAE
- ___ TEA
- ___ photographic developers
- ___ other (list below)

General:

Experiment Class:
- ✓ Base Equipment
- _____ Temp. Mod. to Base Equip.
- _____ Permanent Mod. to Base Equipment
- _____ Major New Apparatus

Other: _____

BEAM REQUIREMENTS LIST

JLab Proposal No.: _____ Date: _____

Hall: C Anticipated Run Date: _____ PAC Approved Days: _____

Spokesperson: O. Keith Baker
Phone: 757-269-7343 or 727-5820
E-mail: baker@cebaf.gov

Hall Liaison: Roger Carlini

List all combinations of anticipated targets and beam conditions required to execute the experiment. (This list will form the primary basis for the Radiation Safety Assesment Document (RSAD) calculations that must be performed for each experiment.)

Condition No.	Beam Energy (MeV)	Mean Beam Current (μA)	Polarization and Other Special Requirements (e.g., time structure)	Target Material (use multiple rows for complex targets — e.g., w/windows)	Material Thickness (mg/cm²)	Est. Beam-On Time for Cond. No. (hours)
1	4.045	35	polarization	liquid hydrogen	280	10.5
2	4.045	35	polarization	dummy Al target		1
3	4.045	35	none	liquid hydrogen	~280	0.5

The beam energies, E_{Beam}, available are: $E_{Beam} = N \times E_{Linac}$ where N = 1, 2, 3, 4, or 5. E_{Linac} = 800 MeV, i.e., available E_{Beam} are 800, 1600, 2400, 3200, and 4000 MeV. Other energies should be arranged with the Hall Leader before listing.

LAB RESOURCES LIST

JLab Proposal No.: _____ Date _____
(For JLab ULO use only.)

List below significant resources — both equipment and human — that you are requesting from Jefferson Lab in support of mounting and executing the proposed experiment. Do not include items that will be routinely supplied to all running experiments such as the base equipment for the hall and technical support for routine operation, installation, and maintenance.

Major Installations *(either your equip. or new equip. requested from JLab)*

N/A

New Support Structures: _____

Data Acquisition/Reduction

Computing Resources: N/A

New Software: _____

Major Equipment

Magnets: N/A

Power Supplies: _____

Targets: _____

Detectors: _____

Electronics: _____

Computer Hardware: _____

Other: _____

Other: _____